

Journal of Materials Chemistry C

Accepted Manuscript



This is an *Accepted Manuscript*, which has been through the Royal Society of Chemistry peer review process and has been accepted for publication.

Accepted Manuscripts are published online shortly after acceptance, before technical editing, formatting and proof reading. Using this free service, authors can make their results available to the community, in citable form, before we publish the edited article. We will replace this *Accepted Manuscript* with the edited and formatted *Advance Article* as soon as it is available.

You can find more information about *Accepted Manuscripts* in the [Information for Authors](#).

Please note that technical editing may introduce minor changes to the text and/or graphics, which may alter content. The journal's standard [Terms & Conditions](#) and the [Ethical guidelines](#) still apply. In no event shall the Royal Society of Chemistry be held responsible for any errors or omissions in this *Accepted Manuscript* or any consequences arising from the use of any information it contains.

Cite this: DOI: 10.1039/c0xx00000x

www.rsc.org/xxxxxx

ARTICLE TYPE

Perylene Crystals: Tuning Optoelectronic Properties By Dimensional-controlled Synthesis

Qing Liao,^{*a} Haihua Zhang,^a Weigang Zhu,^b Ke Hu^a and Hongbing Fu^{*a,b}

Received (in XXX, XXX) Xth XXXXXXXXX 20XX, Accepted Xth XXXXXXXXX 20XX

DOI: 10.1039/b000000x

One-dimensional (1D) ribbon-like and two-dimensional (2D) square-like perylene crystals were controlled prepared via a simple drop casting solution method, by changing the concentration of solution and temperature. Based on SAED and XRD results, both ribbon and square perylene crystals are belong to the α phase. From further optical and electronic characterizations, we find that perylene crystals show unique dimensional-depended optoelectronic properties. In 2D crystal, photons propagate along two edge directions without anisotropy, indicating optical waveguide property may have nothing to do with molecular packing. In comparison, photons propagate along axis direction in 1D crystal seem a little more efficient than that in 2D structure. Moreover, hole mobility of 1D crystal are the same as that along [001] direction of 2D square sheet, while hole carriers transport along two directions of square sheet with anisotropy about 2.3. This is an excellent example which shows optical waveguide and field effect mobility of organic crystal can be tuned by dimensional controlled synthesis.

Introduction

Organic micro-nano crystals¹ with highly order molecular packing have gained a lot of attentions, due to their fundamentally interest and promising applications in miniaturized and multi-functional optoelectronic devices, such as field effect transistor (OFET),^{1, 2} optical waveguide,³ light emitting field effect transistor (LEFET),⁴ sensor,⁵ photodector,⁶ nanolaser,^{7, 8} and solar cell.^{9, 10} Unfortunately, the shapes and dimensions of these crystals obtained from noncovalent self-assembly are not uniformly distributed, thus significantly influence the performance of the devices.¹¹⁻¹⁵ In this regard, polymorphology not only face the problem how to controllably prepare of crystals,¹⁶ but also provide a unique opportunity to explore the structure-function relationship. For opportunities, the behavior of photons and electrons in the one-dimensional (1D), two-dimensional (2D) and three-dimensional (3D) crystals may be completely different, leading to dimensional-depended optoelectronic properties. However, specific relationship between organic crystal dimensional and optoelectronic properties still remain largely elusive.

Among organic small molecules, perylene is a model compound and widely used as a dye molecule. Photoluminescence quantum yield (PLQY) of perylene solution is high up to 89%¹⁷ and the mobility of perylene single crystal (α phase) reach as high as $0.25 \text{ cm}^2\text{V}^{-1}\text{s}^{-1}$.¹⁸ As a matter of fact, perylene molecules can crystallize into two crystal phases¹⁹, α form and β form. Our previous work has declared that perylene crystals show shape and phase depended optical property,¹⁹ but the size of crystal is too small for the measurement of field effect mobility; Ryuzi Katoh and co-workers have reported a growth method of β form crystal,²⁰ but the quality of crystal seems to be not very good. Therefore, controlled preparation of perylene

crystal and systematic study on its dimensional depended optoelectronic properties are still particularly demanded.

Herein, a new shape (1D ribbon-like) and 2D square-like perylene crystals were controllable synthesized, using a simple drop casting solution method, by adjusting the concentration of solution and temperature. The luminescence, optical waveguide and field effect mobility of two perylene crystals have been systematically studied. We find that photons propagate in 1D crystal seem more efficient than that in 2D structure, while hole transportation mobility of ribbon crystal is the same as [001] direction of 2D crystal. Interestingly, photons propagate along two edge directions of 2D crystal without anisotropy, indicating optical waveguide property may have nothing to do with molecular packing. In contrast, the hole mobility along two edge directions of 2D crystal is different. Our work may be helpful for structure-function relationship and controlled preparation of organic crystals.

Results and discussion

Morphology and structure characterization

The square and ribbon of perylene crystals prepared through a simple drop-casting solution method (Experimental Section). Both crystals are as large as $100 \mu\text{m}$ (shown in Figure 1a and b, respectively) with the thickness of hundreds of nanometers, which is ideal for optical and electronic characterization. Especially, the controllable fabrication of large quantities of ribbon perylene crystals on the substrate has been less reported. The photoluminescence (PL) microscopy images of individual perylene crystal are depicted in Figure 1c and d, respectively. Both square sheet and ribbon crystal exhibit a typical yellow emission with PLQY about 0.05. Under excitation of unfocused UV irradiation (330-380 nm), one can also observe that the edges

(or ends of ribbon) of crystals are bright, while the middle part of crystals is dark (Figure 1c and d), implying well self-waveguiding property.

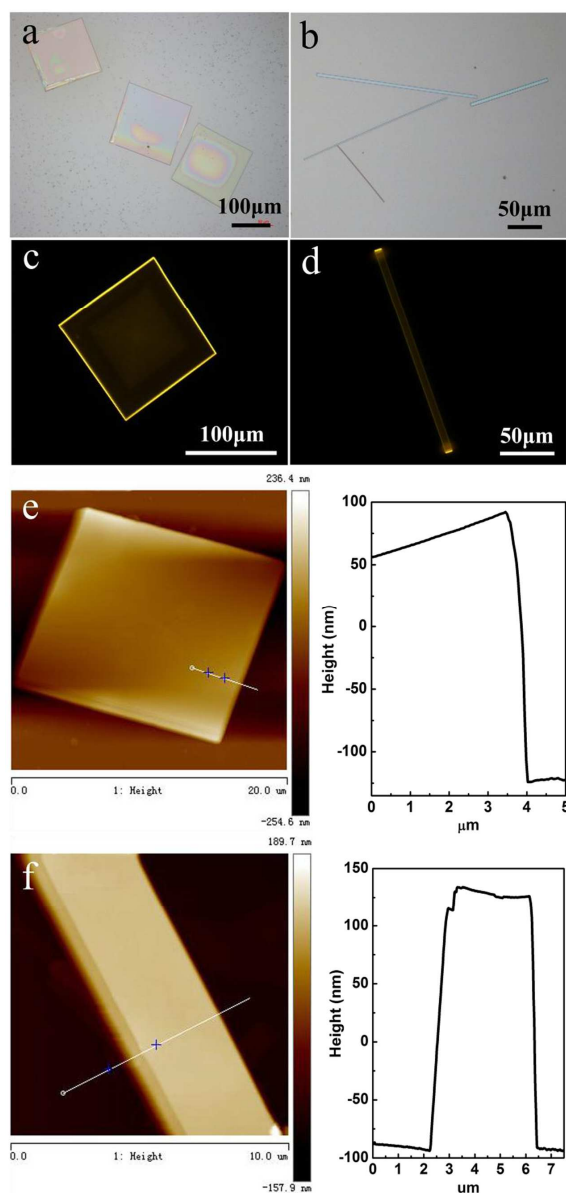


Figure 1. The optical images of (a) square sheet and (b) ribbon crystals; (c) and (d) are PL microscopy images of individual perylene crystal on a glass substrate excited with un-focused UV light (330-380 nm); AFM analysis of (e) square sheet and (f) ribbon crystals

The structure of perylene crystals were confirmed by transmission electron microscope (TEM), select area electron diffraction (SAED) and X-ray diffraction (XRD) results, as shown in Figure 2. It is known that perylene has two phases¹⁹: α form with $a=10.270(1)$, $b=10.839(1)$, $c=11.278(1)$ and $\beta=100.53^\circ$ and β form with $a=11.27$, $b=5.88$, $c=9.65$ and $\beta=92.1^\circ$. Both of them are monoclinic. From the XRD result in Figure 2e, both of square and ribbon crystals belong to α form. A very nice square sheet is depicted in Figure 2a and its corresponding SAED result is shown in Figure 2b. The SAED pattern can be indexed according to the

structure of α form, indicating [010] and [001] are two main growth directions in the square crystal plane, the same as previous report¹⁸. The ribbon crystal depicted in Figure 2c with a width about 3 μm is also attributed to α form after identification of SAED pattern in Figure 2d. One can find [001] is the growth direction of these 1D ribbon crystals, which may be related to the stronger intermolecule interactions (shorter π - π stacking distance), compared with [010] direction.

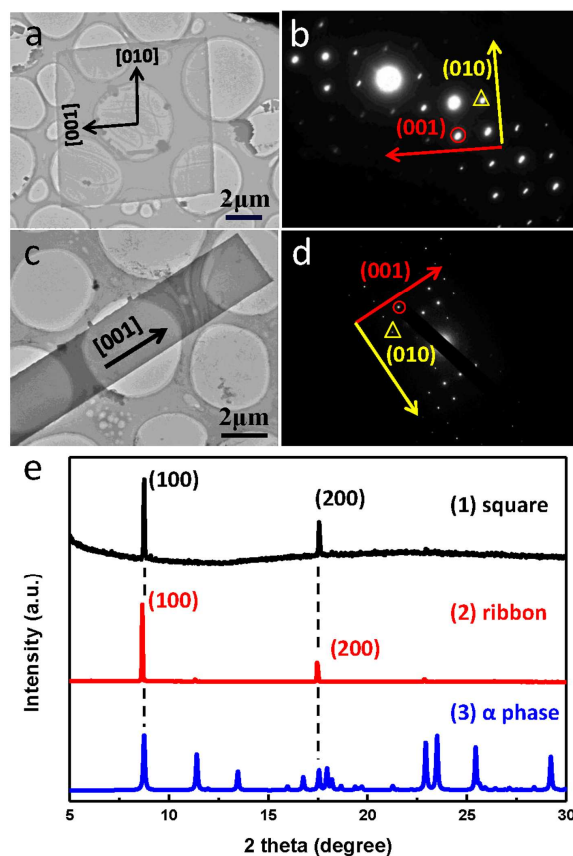


Figure 2. The TEM images of (a) square and (c) ribbon crystals; (b) and (d) are the corresponding SAED patterns; (e) XRD patterns of square (curve 1), ribbon (curve 2) crystals on the substrate and calculated α phase powder (curve 3).

Dimensional-controlled preparation

The shape and dimension of perylene crystals can be well prepared by carefully controlling the experimental conditions including the concentration of perylene acetonitrile solution and temperature, as shown in Table 1. Here, the concentration of solution is the main reason for dimensional control. Square sheet are obtained when the concentration of perylene solution is 1 mM. If smaller concentrations (such as 0.5 mM) are be chosen, no crystals are obtained due to not sufficient molecules for growth of large perylene crystals. However, ribbon crystals are easy to be obtained when saturated perylene acetonitrile solution is used. In the course of crystal growth, π - π interaction is the main driven force and high concentration (saturated) firstly helps overcome the growth barrier along [001] direction, thus ribbon crystal can be obtained. It is noted that the crystal morphology reported here is different from previous report¹⁸, which is due to the

temperature under the drop-casting process.

Temperature is another important factor and helpful to form crystal with different shapes. In our experiment, square sheets were left on the substrate, applying 1 mM perylene acetonitrile solution at room temperature. However, when we dropped the same solution (1 mM) onto the cooled glass substrate, ribbon crystals appeared with small amount of square sheet as a by-product. Meanwhile, square sheets were obtained at high temperature (50 °C) using saturated solution. It can be concluded that high temperature is benefit for two dimensional growth of perylene crystal because low temperature only allow the growth of [001] direction, which possesses lower growth barrier compared with [010] direction.

Therefore, we can control the crystal dimensional by simply changing experiment conditions. Low temperature and high solution concentration is helpful to form ribbon crystal, while high temperature and low solution concentration is beneficial to nucleation and growth of square sheet.

Table 1. Dimensional-controlled preparation of perylene crystals

	Cooled	RT-40 °C	50-60 °C
0.1-0.5 mM	/	/	/
1 mM	ribbon	square	square
saturated	/	ribbon	square

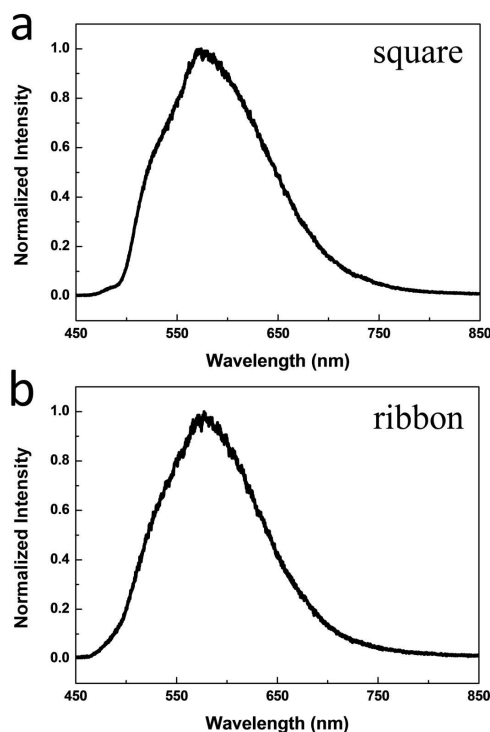


Figure 3. The micro area photoluminescence (PL) spectra of (a) square and (b) ribbon crystals (ex: 408 nm), collected by COM from the laser spot.

PL of crystal

The micro-area PL of perylene crystals were investigated by a home-made confocal optical microscopy (COM) (Figure S1) excited with a 408-nm laser (see the absorption spectrum of perylene film in Figure S2) and the result revealed that the PL spectra of square sheet and ribbon crystal are identical, as depicted in Figure 3. A structureless, broad peak appeared at 580 nm (FWDH about 130 nm) with a shoulder peak at 530 nm in the collected PL spectra. They are assigned to a two-center sandwich excimer (E-type) and a one-center or partial overlapping excimer (Y-type), respectively²¹⁻²³. However, the PL spectra collected from some ribbon crystals with small width (about 2-6 μm) show a series of sharp peaks (Figure S3). This indicates fluorescence resonance phenomenon happens because high-quality cavity are formed in these ribbon crystals. For square sheet, we could not observe the similar PL spectrum even the size of crystal was down to 5 μm.

Waveguide of perylene crystal

To understand the dimensional-depended optical properties of ribbon and square crystals, the optical waveguide measurement was performed by COM under a 408 nm laser beam. When the excitation laser spot moved along ribbon crystal, the ends of ribbon were shining with different PL intensities, as shown in Figure 4a. In this 1D microstructure, photons are confined and propagate oppositely along axis direction of ribbon crystal. Figure 4b and c show that PL intensity collected from tip of ribbon crystal decay with propagation distance increased. The optical propagation loss coefficient (α) measured at 580 nm was calculated to be 72 dB mm⁻¹, according to the waveguide formula (1): $\alpha = -10\log(I_{out}/I_{in})L^{-1}$,²⁴ where I_{out} and I_{in} are the intensities of outcoupled and incidence light, and L is the optical propagation distance.

In comparison, square sheet was excited by laser in the (100) plane and four edges were bright, as shown in Figure 4d. The photons propagate along two directions in this two dimensional structure, providing an opportunity for investigation of waveguide anisotropy in organic crystal. One can see that the PL intensities of four different edges seem to be nearly the same, implying symmetrical waveguide behavior.^{25,26} The PL intensities of edge changed when the laser moved along direction 1, as shown in Figure 4e and f. The optical loss coefficient α was also calculated (99 dB mm⁻¹) according to the formula (1). We performed the same measurement along direction 2 (Figure S4) and found $\alpha = 101$ dB mm⁻¹. This implies no significant difference in optical waveguide property between two directions of square sheet.

The result of optical waveguide property is listed in Table 2. From the experimental results, two points can be conclude: 1) the optical propagation loss coefficient of ribbon crystal is slightly smaller than that of square sheet; 2) the waveguide anisotropy between two directions in square sheet is no different. Based on it, optical waveguide property of perylene crystals is related to the shape or dimension other than molecular packing. In addition, we think that ribbon crystals have less optical propagation loss due to their higher crystal quality.

Cite this: DOI: 10.1039/c0xx00000x

www.rsc.org/xxxxxx

ARTICLE TYPE

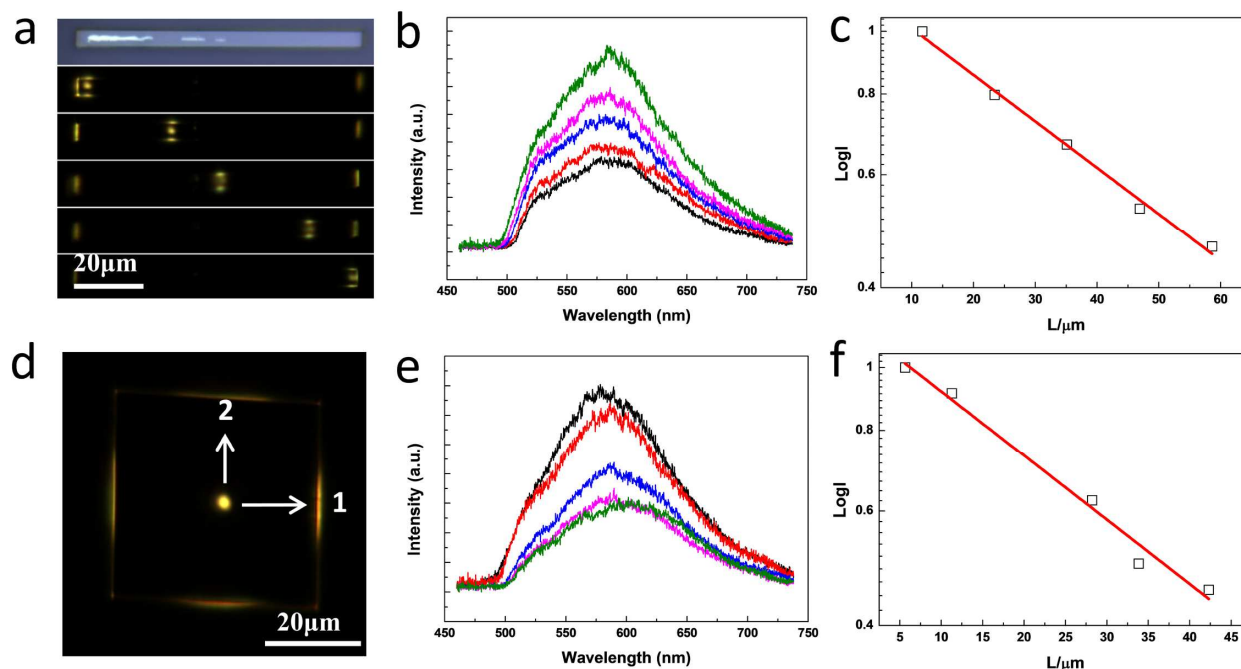


Figure 4. Optical images of individual (a) ribbon and (d) square crystal excited with a 408 nm laser; Waveguide characterizations of (b)-(c) ribbon crystal and (e)-(f) square sheet.

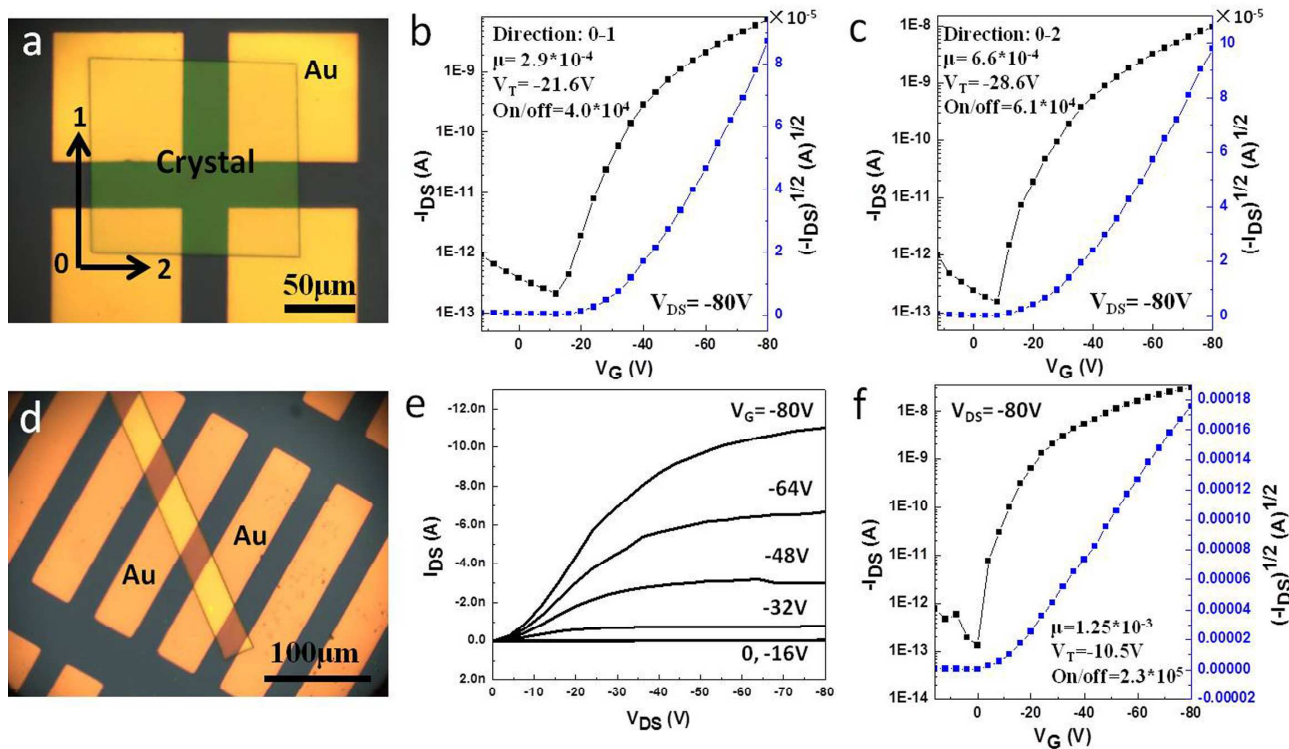


Figure 5. Optical image of (a) square sheet and (d) ribbon crystal; Transfer curves of square sheet (b) along direction 1 and (c) direction 2; (e) output and (f) transfer curves of ribbon crystal.

Cite this: DOI: 10.1039/c0xx00000x

www.rsc.org/xxxxxx

ARTICLE TYPE

Field-effect mobility and anisotropy

To investigate the dimensional depended electronic property, the field effect mobility of ribbon and square crystals were measured, showing little difference. To fabricate of organic single crystal field effect transistor (OFET) device with bottom-gate top-contact geometry, Au source and drain electrodes were thermally evaporated onto crystals using copper grids as the mask. Figure 5a and d show the optical image of perylene crystal based OFET device. More than 20 devices were measured in ambient condition and at room temperature, showing p-type characteristics. The typical output and transfer curves are shown in Figure S5 and the mobility of square sheet was calculated to be $10^{-3} \sim 10^{-4} \text{ cm}^2 \text{ V}^{-1} \text{ s}^{-1}$ (the highest mobility measured was up to $3.6 \times 10^{-3} \text{ cm}^2 \text{ V}^{-1} \text{ s}^{-1}$). The lower mobility from this drop-casting method is attributed to the lower crystal quality, compared with crystal obtained from vapor method in previous report.¹⁸ Two dimensional square crystal is an ideal platform for investigation of intrinsic anisotropy of charge carrier transportation. Figure 5b and c show the transfer curves along two directions of square sheet, respectively. The anisotropy of charge mobility can be calculated to be 2.3. The stronger π - π interaction along [001] is responsible for higher charge carrier mobility and direction 2 is attributed to [001] of perylene crystal (α form).

OFET mobility of ribbon crystals has also been measured for comparison, the result is shown in Figure 5e and f. The mobility of ribbon crystal was calculated to be $1.25 \times 10^{-3} \text{ cm}^2 \text{ V}^{-1} \text{ s}^{-1}$ (the highest mobility measured is up to $2.5 \times 10^{-3} \text{ cm}^2 \text{ V}^{-1} \text{ s}^{-1}$), showing no significant difference with square sheet. In our experiment, the mobility of ribbon crystal was comparable to the direction [001] of square sheet, agreement to structure characterization.

The waveguide and field effect mobility of perylene crystals are listed in the Table 1, clearly showing dimensional depended optoelectronic properties. 1D ribbon crystal can be used as high-performance optoelectronic device with low optical propagation loss and high hole mobility. However, photons propagate in 2D square crystal without anisotropy but hole transport along two directions of crystal with intrinsic anisotropy. This interesting dimension-optoelectronics property of perylene crystals may be widely applied in organic optoelectronics.

Table 2. The optoelectronic properties of perylene crystals

	waveguide (dB· μm^{-1})	waveguide anisotropy	μ_{max} ($\text{cm}^2 \text{ V}^{-1} \text{ s}^{-1}$)	mobility anisotropy
ribbon	0.07	/	2.5×10^{-3}	/
square	0.1	1	3.6×10^{-3}	2.3

Conclusions

In summary, perylene 1D ribbon-like and 2D square-like crystals have been controllable synthesised by altering experimental

conditions. Low temperature and high solution concentration is helpful to form ribbon crystal, while high temperature and low solution concentration is beneficial to nucleation and growth of square sheet. Further structure characterizations confirm that both crystals are belong to the α form. From the results of waveguide characterization, we find optical waveguide property has nothing to do with molecular packing but somehow related to the shape (dimensional) of crystal. Photons propagate in 1D crystal seem a little more efficient than that in 2D structure, while hole mobility of 1D crystal is the same as that along [001] direction of 2D square sheet. Moreover, hole carriers transport along two directions of square sheet with mobility anisotropy about 2.3. This work shows that optical waveguide and field effect mobility of organic crystal can be tuned by dimensional-controlled synthesis.

Experimental**Chemicals and materials**

Perylene ($\text{C}_{20}\text{H}_{12}$, 99.5%) was pursued from Sigma-Aldrich Co. and directly used without further purification; Acetonitrile (CH_3CN , HPLC) was pursued from Beijing Chemical Co. China.; Clear glass substrates (size 22×22 mm) were pursued from Electron Microscopy Sciences (EMS); Deionized water ($18.2 \text{ }\Omega\text{M}\cdot\text{cm}^{-1}$) was made by a Milli-Q (Millipore) water purification system.

Preparation of perylene crystals

For ribbon crystal, several drops of saturated perylene acetonitrile solution were directly deposited onto the substrate (glass, SiO_2/Si or copper grid) and the solvent evaporated in the room temperature. For square crystal, 1 mM perylene solution and the substrate heated to 120 °C were necessary conditions. For low temperature experiments, the substrates were firstly placed in the icebox (0 °C) for a period time, then were taken out directly for use.

Characterization

TEM and SAED were performed on a JEOL JEM-1011 electron microscope at an acceleration of 100 kV to gain a sufficient transmission. For optical characterization, PL microscopy images of samples were recorded on a glass substrate using an Olympus research inverted system microscope (FV1000-IX81, Tokyo, Japan) equipped with a charge couple device (CCD, Olympus DP71, Tokyo, Japan) camera. The excitation source is a Xenon lamp equipped with a band-pass filter (330–380 nm). Micro-area PL measurement was performed on a home-made optical microscopy. Perylene crystals were excited with a continuous-wave laser ($\lambda = 408 \text{ nm}$) and PL spectra were coupled into an optical fiber and collected using a liquid nitrogen cooled CCD (SPEC-10-400B/LbN, Roper Scientific) attached to a polychromator (Spectropro-550i, Acton).

For electronic characterization, we used highly n-doped (100

Si wafers (0.05-0.2 Ωcm) with a 300 nm SiO_2 as dielectric layer (10 nFcm⁻²). The SiO_2/Si substrates were firstly washed by acetone, ethanol, deionized water and hot sulfuric acid:hydrogen peroxide = 7:3 solution and dried by a N_2 gun. Perylene crystals were fabricated by directly dropping the perylene/acetone nitrile solution onto the silicon wafers, the same as glass substrate. The crystals were further annealed in vacuum oven for at least 2H to remove the solvent. A top-contact/bottom gate configuration was used to fabricate the perylene crystal based OFET device. The source and drain electrodes (Au, 40 nm thick) were evaporated and copper grids were used as mask. The current-voltage (*I-V*) curves were recorded with a Keithley 4200 SCS analyzer. All measurements were performed at room temperature in air.

15 Acknowledgement

This work was supported by the National Natural Science Foundation of China (Nos. 21073200, 21273251, 91333111, 21190034, 21221002), Project of Construction of Innovative Teams and Teacher Career Development for Universities and Colleges Under Beijing Municipality (IDHT20140512), the National Basic Research Program of China (973) 2011CB808402, 2013CB933500, and the Chinese Academy of Sciences.

Notes and references

^a Beijing Key Laboratory for Optical Materials and Photonic Devices,

²⁵ Department of Chemistry, Capital Normal University, Beijing, 100048, P. R. China. Tel: +86-10-82616517; E-mail: liaoping@cnu.edu.cn; Hongbing.Fu@iccas.ac.cn

^b Beijing National Laboratory for Molecular Sciences (BNLMS), Institute of Chemistry, Chinese Academy of Sciences, Beijing, 100190. E-mail: hongbing.fu@iccas.ac.cn

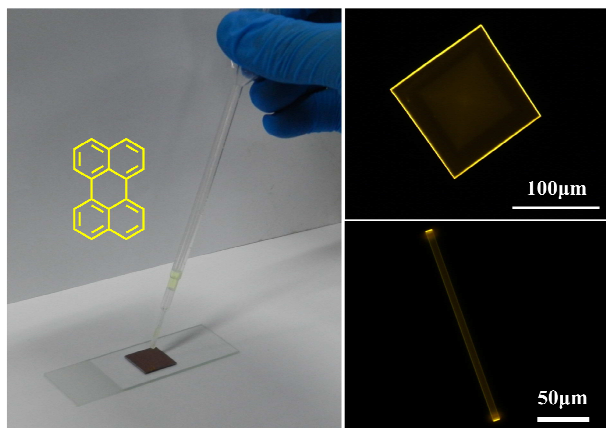
† Electronic Supplementary Information (ESI) available: [details of any supplementary information available should be included here]. See DOI: 10.1039/b000000x/

‡ Footnotes should appear here. These might include comments relevant to but not central to the matter under discussion, limited experimental and spectral data, and crystallographic data.

1. R. Li, W. Hu, Y. Liu and D. Zhu, *Acc. Chem. Res.*, 2010, **43**, 529-540.
2. T. He, M. Stolte and F. Würthner, *Adv. Mater.*, 2013, n/a-n/a.
3. Y. S. Zhao, H. Fu, A. Peng, Y. Ma, Q. Liao and J. Yao, *Acc. Chem. Res.*, 2009, **43**, 409-418.
4. S. Z. Bisri, T. Takenobu, Y. Yomogida, H. Shimotani, T. Yamao, S. Hotta and Y. Iwasa, *Adv. Funct. Mater.*, 2009, **19**, 1728-1735.
5. L. Zang, Y. Che and J. S. Moore, *Acc. Chem. Res.*, 2008, **41**, 1596-1608.
6. Y. Zhou, L. Wang, J. Wang, J. Pei and Y. Cao, *Adv. Mater.*, 2008, **20**, 3745-3749.
7. M. Ichikawa, R. Hibino, M. Inoue, T. Haritani, S. Hotta, K. Araki, T. Koyama and Y. Taniguchi, *Adv. Mater.*, 2005, **17**, 2073-2077.
8. Z. Xu, Q. Liao, Q. Shi, H. Zhang, J. Yao and H. Fu, *Adv. Mater.*, 2012, **24**, OP216-OP220.
9. Q. H. Cui, L. Jiang, C. Zhang, Y. S. Zhao, W. Hu and J. Yao, *Adv. Mater.*, 2012, **24**, 2332-2336.
10. Y. Zhang, H. Dong, Q. Tang, S. Ferdous, F. Liu, S. C. B. Mannsfeld, W. Hu and A. L. Briseno, *J. Am. Chem. Soc.*, 2010, **132**, 11580-11584.
11. L. Huang, Q. Liao, Q. Shi, H. Fu, J. Ma and J. Yao, *J. Mater. Chem.*, 2010, **20**, 159-166.
12. J. Wang, Y. Zhao, J. Zhang, J. Zhang, B. Yang, Y. Wang, D. Zhang, H. You and D. Ma, *J. Phys. Chem. C*, 2007, **111**, 9177-9183.
13. Y. Liu, Z. Ji, Q. Tang, L. Jiang, H. Li, M. He, W. Hu, D. Zhang, L. Jiang, X. Wang, C. Wang, Y. Liu and D. Zhu, *Adv. Mater.*, 2005, **17**, 2953-2957.

14. J. W. Lee, K. Kim, J. S. Jung, S. G. Jo, H.-m. Kim, H. S. Lee, J. Kim and J. Joo, *Organic Electronics*, 2012, **13**, 2047-2055.
15. H.-X. Ji, J.-S. Hu, L.-J. Wan, Q.-X. Tang and W.-P. Hu, *J. Mater. Chem.*, 2008, **18**, 328-332.
16. J. Bernstein, R. J. Davey and J.-O. Henck, *Angew. Chem. Int. Ed.*, 1999, **38**, 3440-3461.
17. S. J. Strickler and R. A. Berg, *J. Chem. Phys.*, 1962, **37**, 814-822.
18. H. Jiang, K. K. Zhang, J. Ye, F. Wei, P. Hu, J. Guo, C. Liang, X. Chen, Y. Zhao, L. E. McNeil, W. Hu and C. Kloc, *Small*, 2013, **9**, 990-995.
19. Y. Lei, Q. Liao, H. Fu and J. Yao, *J. Phys. Chem. C*, 2009, **113**, 10038-10043.
20. T. Yago, Y. Tamaki, A. Furube and R. Katoh, *Chem. Lett.*, 2007, **36**, 370-371.
21. L. Kang, Z. Wang, Z. Cao, Y. Ma, H. Fu and J. Yao, *J. Am. Chem. Soc.*, 2007, **129**, 7305-7312.
22. S. Akimoto, A. Ohmori and I. Yamazaki, *The Journal of Physical Chemistry B*, 1997, **101**, 3753-3758.
23. D. Weiss, R. Kietzmann, J. Mahrt, B. Tufts, W. Storck and F. Willig, *J. Phys. Chem.*, 1992, **96**, 5320-5325.
24. Q. Liao, H. Fu, C. Wang and J. Yao, *Angew. Chem. Int. Ed.*, 2011, **50**, 4942-4946.
25. W. Yao, Y. Yan, L. Xue, C. Zhang, G. Li, Q. Zheng, Y. S. Zhao, H. Jiang and J. Yao, *Angew. Chem. Int. Ed.*, 2013, **52**, 8713-8717.
26. L. Heng, X. Wang, D. Tian, J. Zhai, B. Tang and L. Jiang, *Adv. Mater.*, 2010, **22**, 4716-4720.

TOC figure



5